PLOS ONE

RESEARCH ARTICLE

Isolating and cryopreserving pig skin cells for single-cell RNA sequencing study

Li Han[1,2,3,4☯], Carlos P. Jara[5,6☯], Ou Wang[2], Yu Shi[1], Xinran Wu[3,4], Sandra Thibivilliers[7], Rafał K. Wóycicki[7], Mark A. Carlson[8,9], William H. Velander[2], Eliana P. Araújo[5,6], Marc Libault[7]*, Chi Zhang[1]*, Yuguo Lei[2,3,4,8,9,10]*

1 School of Biological Science, University of Nebraska, Lincoln, Nebraska, United States of America, 2 Department of Chemical and Biomolecular Engineering, University of Nebraska, Lincoln, Nebraska, United States of America, 3 Department of Biomedical Engineering, Pennsylvania State University, University Park, Pennsylvania, United States of America, 4 Huck Institutes of the Life Sciences, Pennsylvania State University, University Park, Pennsylvania, United States of America, 5 Nursing School, University of Campinas, Campinas SP, Brazil, 6 Laboratory of Cell Signaling, University of Campinas, Campinas SP, Brazil, 7 Department of Agronomy and Horticulture, Center for Plant Science Innovation, University of Nebraska, Lincoln, Nebraska, United States of America, 8 Mary and Dick Holland Regenerative Medicine Program, University of Nebraska Medical Center, Omaha, Nebraska, United States of America, 9 Department of Surgery, University of Nebraska Medical Center and the VA Nebraska-Western Iowa Health Care System, Omaha, Nebraska, United States of America, 10 Sartorius Mammalian Cell Culture Facility, Pennsylvania State University, University Park, Pennsylvania, United States of America

☯ These authors contributed equally to this work.
* marc.libault@unl.edu (ML); zhang.chi@unl.edu (CZ); yxl6034@psu.edu (YL)

Abstract

The pig skin architecture and physiology are similar to those of humans. Thus, the pig model is very valuable for studying skin biology and testing therapeutics. The single-cell RNA sequencing (scRNA-seq) technology allows quantitatively analyzing cell types, compositions, states, signaling, and receptor-ligand interactome at single-cell resolution and at high throughput. scRNA-seq has been used to study mouse and human skins. However, studying pig skin with scRNA-seq is still rare. A critical step for successful scRNA-seq is to obtain high-quality single cells from the pig skin tissue. Here we report a robust method for isolating and cryopreserving pig skin single cells for scRNA-seq. We showed that pig skin could be efficiently dissociated into single cells with high cell viability using the Miltenyi Human Whole Skin Dissociation kit and the Miltenyi gentleMACS Dissociator. Furthermore, the obtained single cells could be cryopreserved using 90% FBS + 10% DMSO without causing additional cell death, cell aggregation, or changes in gene expression profiles. Using the developed protocol, we were able to identify all the major skin cell types. The protocol and results from this study are valuable for the skin research scientific community.

Introduction

Millions of people are affected by skin injuries and diseases [1–3]. Animal models are widely used to understand skin physiopathology and to test potential therapeutics [4,5]. Among various experimental animals, the skin architecture and physiology of pigs are closest to humans

[6–8]. FDA thus recommends including pigs for pre-clinical biology study and therapeutic testing [9,10]. Conventionally, the skin is investigated using low-content technologies such as qPCR, flow cytometry, and histology. The most recently developed single-cell RNA sequencing (scRNA-seq) technology allows simultaneously and quantitively analyzing the transcriptome of thousands of individual cells. It leads to new insights into the cell types, compositions, states, signaling, receptor-ligand interactome, and their dynamics during development, disease, and treatment [11–13]. Additionally, when combined with the high-content immunostaining and fluorescent imaging [14], or the cutting-edge Spatial Transcriptomics technology [11–13], the spatial and temporal organization of these cells and their interactions can also be obtained. scRNA-seq has been used to study rodent [15–22] and human [13,21,23–30] skins. However, using scRNA-seq to study pig skin is still rare.

In a typical scRNA-seq workflow, tissues are first dissociated into single cells (i.e., the upstream single cell preparation). These freshly isolated cells are then used to prepare RNA libraries using droplet-based technology (i.e., the downstream library preparation) [31]. The libraries are then sequenced using the deep sequencing technology [32]. Preparing high-quality single cells is critical for the success of the downstream process. Partial or incomplete tissue dissociation, cell aggregation, and cell death should be avoided during the preparation.

Recently studies showed that adding a cell preservation step between the upstream single cell preparation and downstream RNA library construction makes the scRNA-seq workflow much more flexible, manageable, and accessible to researchers [24,33–36]. First, some research facilities/institutions do not have the infrastructure and expertise to prepare scRNA-seq libraries for the freshly isolated cells. Instead, they ship cells to service facilities for RNA library construction and sequencing. Cells should be preserved during shipping. Second, most studies collect samples at multiple time points and different locations. Preparing RNA libraries at the same facilities can increase consistency and reduce experimental variations. To achieve this, cells need preservation. A suitable cell preservation method should not significantly change the cell viability, composition, and gene expression [24,33–36]. To our best knowledge, there have been no reports on how to prepare and preserve single cells from pig skin tissues for scRNA-Seq, which this study aims to address.

Materials and methods

Harvesting pig skin

Fresh skin tissues from healthy farm male pigs with about 30 kg of body weight were provided by the University of Nebraska-Lincoln Swine Facility. The Institutional Animal Care and Use Committee of the University of Nebraska-Lincoln granted a waiver of ethics approval for using skins harvested from dead animals. The dorsal area of the skin was washed with PBS, and the fur was removed with a disposable scalpel. The skin was disinfected with 70% ethanol, harvested using sterile scissors, and stored in the MACS Tissue Storage Solution (Miltenyi Biotech Inc) with 1% Antibiotic-Antimycotic (ThermoFisher Scientific). The samples were kept on ice and transported to the lab for single cell isolation.

Isolating single cells

The skin was washed with sterile iced cold PBS three times, and the subcutaneous fat was scraped off using a scalpel. A full skin sample, including the epidermis and dermis, was taken with a 4-mm diameter punch. The sample was then dissociated using the Human Whole Skin Dissociation Kit (Miltenyi Biotech Inc). Briefly, 435 µL of Buffer L and 12.5 µL of Enzyme P were put into a gentleMACS C tube and gently mixed before adding 50 µL of Enzyme D and 2.5 µL of Enzyme A. One skin sample was placed into the tube and incubated at 37°C for three

hours. The tube was inverted for mixing every ten minutes. The enzymatic reaction was stopped by adding 0.5 mL ice-cold cell culture medium (DMEM + 10%FBS). The sample was then mechanically dissociated with a gentleMACS Dissociator (Miltenyi Biotech Inc) using the "h_skin_01" program. The suspension was passed through a 70 μm strainer to remove tissue debris, if any. Cells were collected by centrifugation at 300 g for 5 minutes. The supernatant was aspirated, and the cell pellet was resuspended in 5 mL DMEM + 10% FBS. Cells were counted using a Countess II FL Automated Cell Counter (ThermoFisher Scientific) on a 0.2% trypan blue staining. The viability was further assessed using the LIVE/DEAD™ Viability/Cyto-toxicity Kit for mammalian cells (Invitrogen).

Cryopreserving cells

The freshly isolated cell suspension was centrifuged at 300 g for 5 minutes. The cell pellet was resuspended with FBS containing 10% DMSO at $1x10^6$ cells/mL. Next, 1 mL cells suspension was put in a cryopreservation vial and placed in a Mr. Frosty Freezing Container (Thermo-Fisher Scientific). The container was placed in a -80˚C freezer overnight before being stored in liquid N_2 for the long term.

Thawing cells

The frozen vial was removed from the liquid N_2 storage and placed in a 37˚C water bath. After thawing, the cell suspension was centrifuged at 300 g for 5 minutes and resuspended in DMEM + 10% FBS. The cell viability was assessed with the LIVE/DEAD™ Viability/Cytotoxic-ity Kit and flow cytometer.

Removing dead cells and cell aggregates using Fluorescence-Activated Cell Sorting (FACS)

4 μL of 2 mM ethidium homodimer-1 was added to each milliliter cell suspension and incu-bated for 20 minutes at room temperature to stain the dead cells before sorting (FACSAriaII). Side-scatter and forward-scatter profiles were used to eliminate cell doublets. Living cells were gated as ethidium homodimer-1 negative. The sorted cells were re-analyzed for purity using a flow cytometer. Data were analyzed with BD FACS Diva software.

Removing dead cells using Magnetic-Activated Cell Sorting (MACS)

An alternative approach was used to remove dead cells with the Dead Cell Remove Kit (Milte-nyi Biotech Inc) following the product instruction. Briefly, the cell suspension was centrifuged at 300 g for 5 minutes. Cells were resuspended in 100 μL of Dead Cell Removal MicroBeads and incubated for 15 minutes at room temperature. Dead cells were removed using a MACS Separator (Miltenyi Biotech Inc) following the product instruction.

Library construction

Cells were suspended in DMEM+10% FBS. The cells' density and viability were estimated using a Countess II FL Automated Cell Counter. About 8,000 cells were used as the input to generate an RNA-seq library following the 10X Genomics Chromium Next GEM Single Cell 3′ kit V3 protocol. Libraries were sequenced at Novogene using NovaSeq 6000 sequencer.

Data processing

scRNA-seq data was processed with Cell Ranger pipeline version 4.0.0. (10x Genomics). A ref-erence transcriptome was created by utilizing the pig reference genome (Sscrofa11.1) and its

annotation downloaded from Ensemble (https://www.ensembl.org/Sus_scrofa/Info/Index).
The reads were mapped using STAR aligner (v. 2.5.1b) against the reference transcriptome to
detect and count UMIs and expressed genes.

Data analysis

The quality of sequencing data was assessed using quality control parameters, including the
gene counts per cell, UMI counts per cell, and mitochondrial gene expression [37,38]. These
quality control parameters were calculated as part of the scRNA-seq data analysis procedure
using the Seurat R package version 3.2.1 [37]. Since cell doublets or multiplets exhibit an aber-
rantly high gene and molecule counts, we set a maximum threshold at 4,500 genes per cell and
30,000 molecules per cell (S1 Fig). Also, we allowed cells up to 10% mitochondrial gene expres-
sion (S1 Fig).

The sample data sets were merged into one R Data object per experiment for joint cluster
analysis. Then, the UMI count data per cell were normalized and log-transformed using the
default settings of the "Normalize Data" function in Seurat [37]. Principal component analysis
(PCA) was performed using the highly variable genes for each sample. Significant principal
components were selected for subsequent cluster analysis. Single cell clustering was visualized
with uniform manifold approximation and projection (UMAP) plots with default parameters.
Cell types were annotated using marker genes with at least a 2-fold increase in individual cell
clusters compared to the remaining cells. We used CellMatch for automated cell type annota-
tion [39]. Based on the evidence-based score, we annotated the clusters by matching the identi-
fied marker genes with known cell markers in tissue-specific cell taxonomy reference
databases [39]. For single-cell trajectory analysis [40,41], we used an algorithm to learn the
changes in each cell's gene expression sequence. Once the algorithm has learned the overall
"trajectory" of gene expression changes, we placed each cell at its proper position in the trajec-
tory (line).

Statistically significant differences between cell cluster gene levels were calculated using the
MAST linear model approach, as implemented in the Seurat package. Genes were considered
as being significantly altered if gene expression levels had at least 2-fold changes and adjusted
P-values were less than 0.001 (Bonferroni correction). The overall similarity of fresh and cryo-
preserved samples' gene expression profiles was assessed by the correlation performed on
"pseudo-bulk" expression profiles [42], which were generated by summing counts together for
all cells within the same sample by using the function of "*aggregateAcross*" in the Scatter pack-
age [43]. The raw pseudo-bulk count matrices were normalized using edgeR version 3.30.3
[44]. Pearson correlation of the fresh and cryopreserved samples was computed using the nor-
malized counts. The differentially expressed pseudo-bulk genes were identified by edgeR.

Statistical analysis

The data are presented as the mean ± S.D. We used an unpaired t-test to compare two groups
and one-way ANOVA to compare more than two groups. P-value < 0.05 was considered sta-
tistically significant. We used GraphPad Prism 6 for Windows 6.01v to perform statistical
analysis.

Results

Isolating and preserving single pig skin cells

We used the Miltenyi Human Whole Skin Dissociation Kit and the gentleMACS Dissociator
to dissociate the pig skin. Our results showed the combination efficiently dissociated the skin
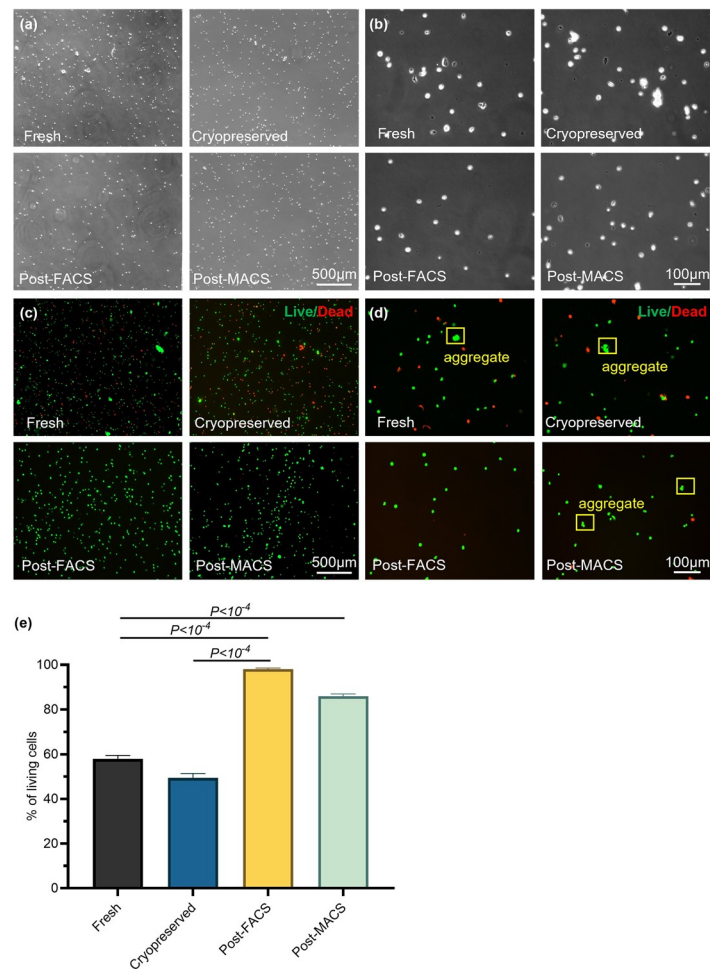
Fig 1. Efficient single cell preparation. Phase (a, b), live/dead staining (c, d), and flow cytometry viability quantification (e) of fresh isolated, cryopreserved, post-FACS, and post-MACS pig skin cells. n = 3 for (e).

into single cells with only a few cell aggregates and no cell or tissue debris. The resultant cells had healthy and spherical morphology (Fig 1A and 1B). Live/dead cell staining showed that most cells were live, and confirmed cell aggregates were few (Fig 1C and 1D). Flow cytometry analysis showed that >60% of cells were viable (Fig 1E). We froze the freshly isolated cells in 90% FBS + 10% DMSO at -80˚C, followed by long-term storage in liquid N_2. After thawing, cryopreserved cells had similar spherical morphology and viability as the fresh cells (Fig 1A–1E), preliminarily indicating this method is appropriate for preserving cells. Furthermore, the cryopreservation did not induce cell aggregation.

Cell aggregates interfere with the downstream library preparation. RNAs released from dead cells negatively affect scRNA-seq results. We sought to remove both aggregated and dead cells with fluorescence-activated cell sorting (FACS) before the library preparation. Dead cells were stained with ethidium homodimer-1 dye and removed via the red fluorescence. Cell doublets were removed using the side-scatter and forward-scatter profiles. FACS quantitively removed both (Fig 1D). Since many researchers have difficulty accessing a FACS instrument, we also used an alternative and compact device, the Miltenyi magnetic-activated cell sorting (MACS), to remove the dead cells. MACS quantitively removed dead cells. However, it was not efficient to remove cell aggregates (Fig 1D). In summary, it is appropriate to combine the

Human Whole Skin Dissociation Kit, the gentleMACS Dissociator, cryopreservation, and FACS to prepare and preserve high-quality single pig skin cells for scRNA-seq.

Cryopreservation in 90% FBS + 10% DMSO preserved gene expression

Our data showed the genes per cell, UMIs per cell, % mitochondrial genes were similar between the fresh and the cryopreserved sample (Fig 2A–2C). The pseudo-bulk expression
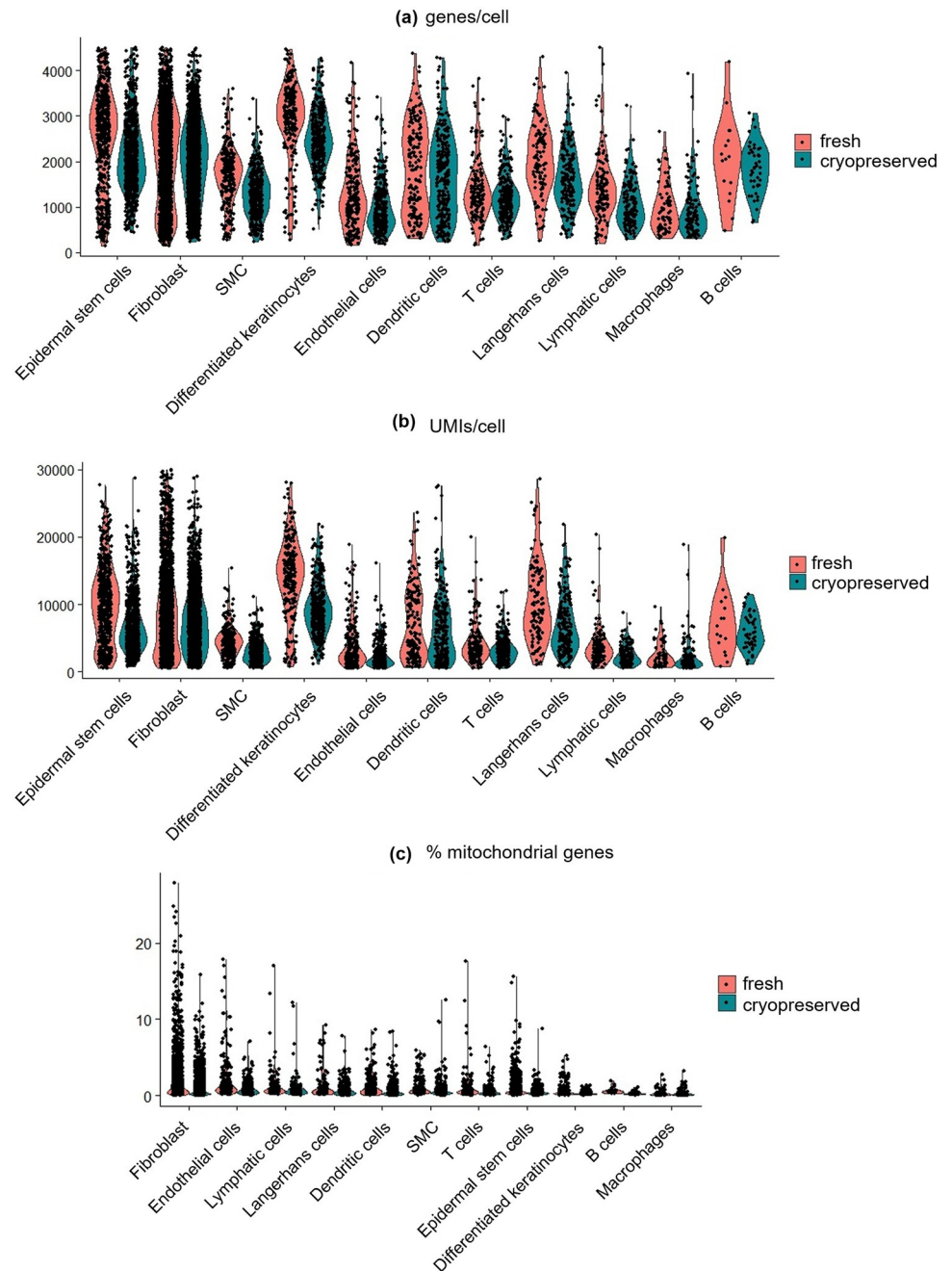

Fig 2. Fresh and cryopreserved cells have similar quality control parameters. The genes per cell (a), UMIs per cell (b), and % mitochondrial genes (c) in each cell of fresh and cryopreserved samples by cell type. Each dot represents one cell.
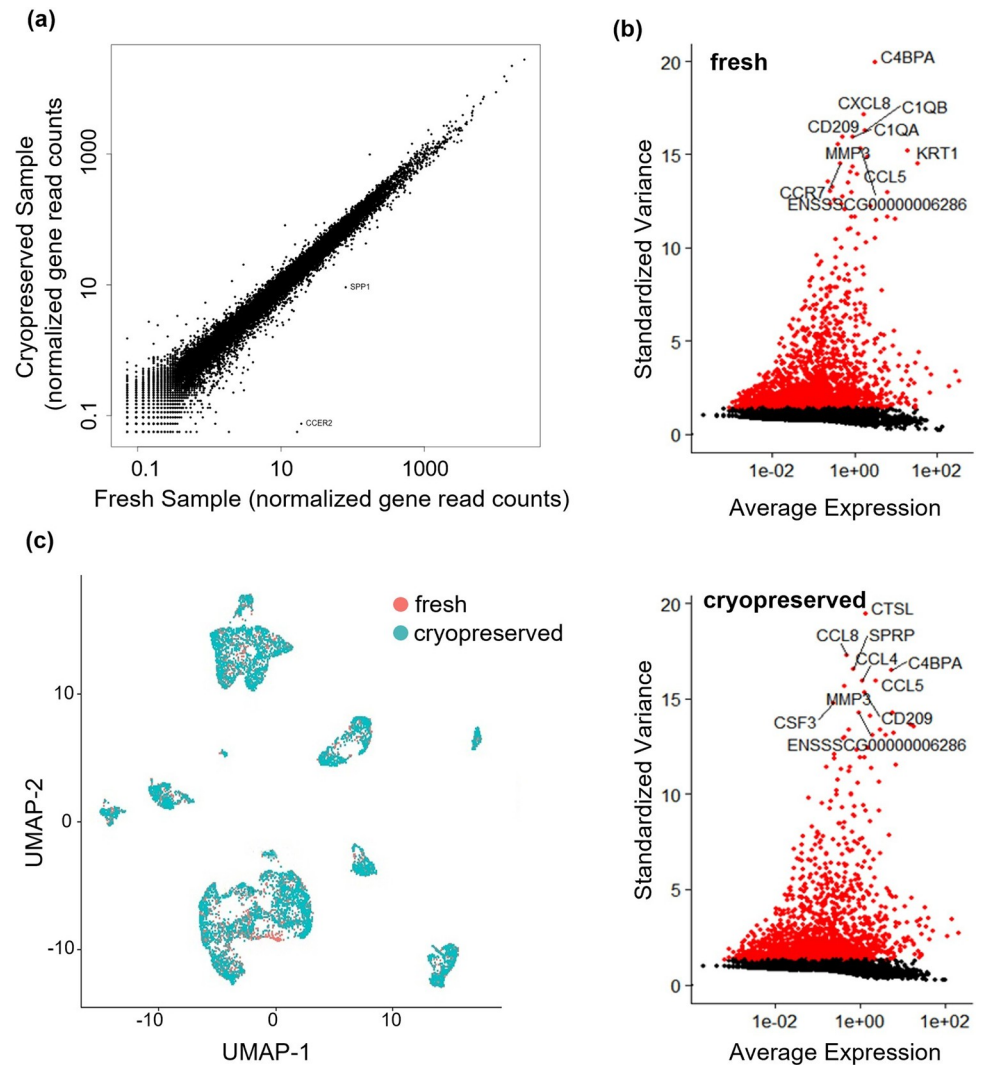
https://doi.org/10.1371/journal.pone.0263869.g002

Fig 3. Fresh and cryopreserved cells have similar gene expression profiles. (a) The pseudo-bulk expression profiles of fresh and cryopreserved cells are compared using correlation scatter plots. The profiles correlate well (R = 0.981). (b) Analysis of the highly variable genes shows fresh and cryopreserved samples share the highly variable features with similar variance and average expression. (c) UAMP shows fresh and cryopreserved samples have similar structures.

profiles of cryopreserved and fresh cells were compared using correlation analysis to assess if cryopreservation alters the gene expression. The expression profile of the cryopreserved sample correlated very well with this of fresh cells (R = 0.981) (Fig 3A). Among 20,428 expressed genes, there were only 57 differentially expressed genes (DEGs) between fresh and cryopreserved samples with FDR adjusted P-values < 0.01. This indicates the gene expression profiles between fresh and cryopreserved samples are almost the same. Next, we analyzed the subset of genes that exhibited high cell-to-cell variation in the samples (Fig 3B). Fresh and cryopreserved samples shared the highly variable features (e.g., CD209, MMP3, CCL5, C4BPA) with similar variance and average expression. Lastly, we assembled the fresh and the cryopreserved sample into an integrated reference and visualized the integration using a non-linear dimensional reduction UMAP (Fig 3C). Again, the fresh and cryopreserved cells formed similar structures. These results show that cryopreservation in 90% FBS + 10% DMSO did not alter the gene expression significantly.

Cryopreservation in 90% FBS + 10% DMSO retained the major skin cell types

Next, we sought to answer if the single cell preparation protocol could retain the major skin cell types and if the cryopreservation changed the cell composition. We performed a clustering analysis of the integrated cryopreserved and fresh cells using a graph-based clustering approach [37,45]–the Louvain algorithm [46]. This method embeds cells in a graph structure, clusters cells with similar feature expressions, and partitions the graph into highly interconnected communities. We identified 18 clusters (S2 Fig) and the top 10 marker genes for each cluster (S3 Fig). We then used a mixed strategy to annotate the clusters. We used CellMatch [46] to annotate clusters based on the evidence-based score by matching the identified marker genes with known cell markers in tissue-specific cell taxonomy reference databases. Also, we used cell marker genes from recent scRNA-seq studies of skin [16,27] to identify the remaining cell types. This allows us to identify the major skin cell types (Fig 4A). The expression levels for the markers of each cell type were shown in Fig 5 and S1 Table. The top 10 marker genes for each cell type were also identified (S4 Fig). We compared the fresh and the cryopreserved samples regarding the relative organization and connection between cell clusters (Fig 4A). The two
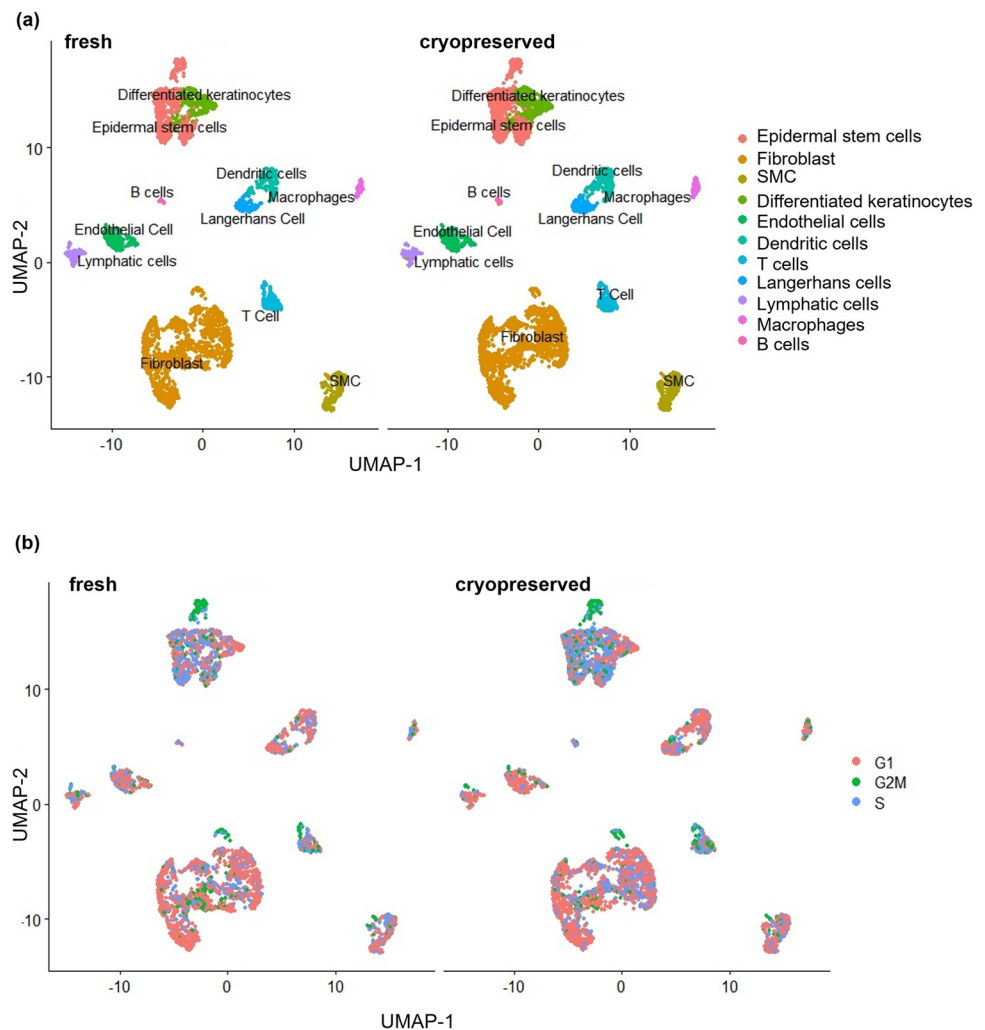

Fig 4. Fresh and cryopreserved samples have similar cell types (a) and cell cycle status (b).

https://doi.org/10.1371/journal.pone.0263869.g004

Table 1. Cellular composition in fresh and cryopreserved samples.

Cell type	cryopreserved	fresh
Epidermal stem cells	17.8%	16.0%
Fibroblast	37.9%	45.5%
SMC	8.2%	7.2%
Differentiated keratinocytes	7.7%	6.7%
Endothelial cells	6.3%	6.5%
Dendritic cells	5.9%	4.6%
T cells	5.5%	4.3%
Langerhans cells	4.1%	3.1%
Lymphatic cells	2.9%	3.3%
Macrophages	2.5%	2.1%
B cells	0.9%	0.4%

https://doi.org/10.1371/journal.pone.0263869.t001

samples were very similar. Also, the cryopreservation did not significantly alter the cell compositions (Table 1).

Cryopreservation retained the cell cycle status and differentiation trajectory

Further, we used cell cycle regression to analyze the effect of cryopreservation on the cell cycle status. We identified the cell cycle heterogeneity from cryopreserved and fresh samples by calculating cell cycle phase scores based on canonical markers [39]. Our results showed no differences between fresh and cryopreserved keratinocytes regarding G2/M-phase genes (Fig 4B). Using the single-cell trajectory analysis [40,41], we found that epidermal stem cells differentiated into keratinocytes in both fresh and cryopreserved samples (Fig 6A and 6B). The results indicate the data quality for both the fresh and cryopreserved cells is sufficient for transcriptional trajectory analysis.

Discussion

Preparing high-quality single cells is a critical step for a successful scRNA-seq study. A suitable dissociation method should dissolve the whole skin tissue, including epidermis and dermis, to
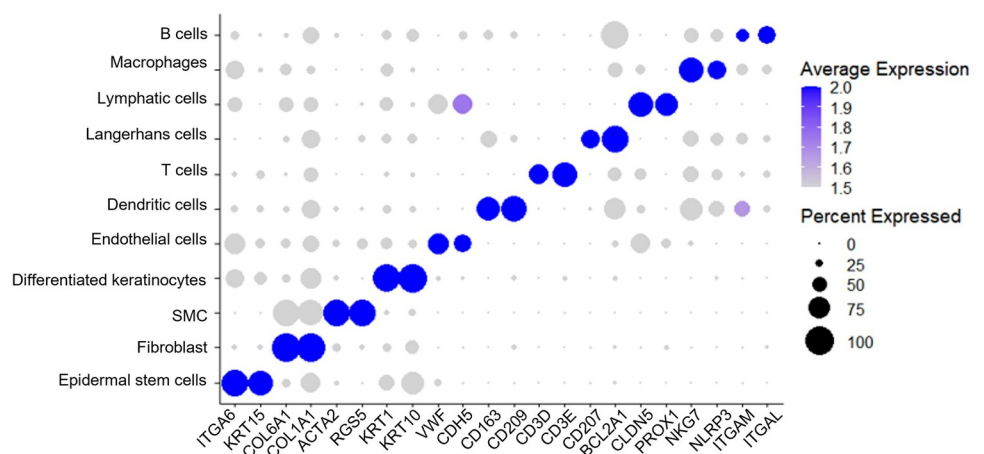

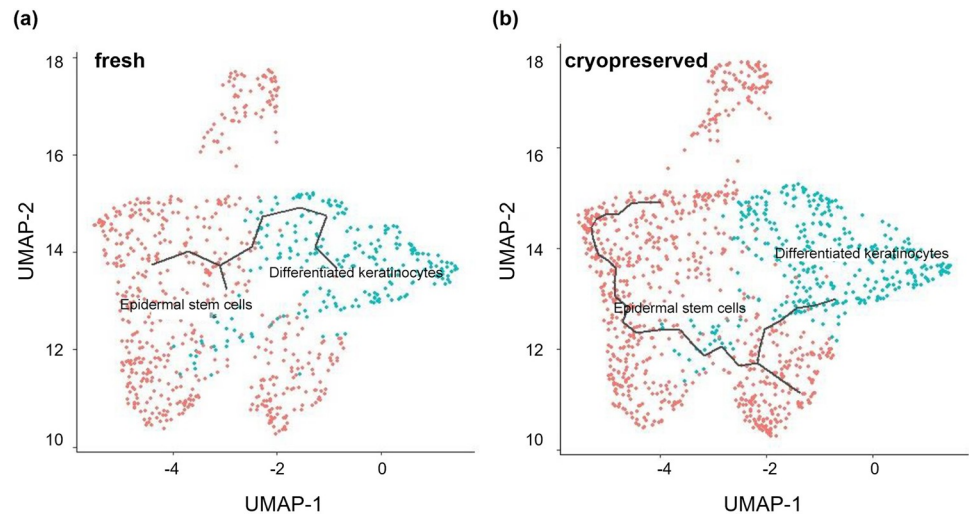**Fig 5. Dot plot of marker genes for pig skin cells.**

https://doi.org/10.1371/journal.pone.0263869.g005

Fig 6. Single-cell trajectory analysis shows epidermal stem cells differentiate into keratinocytes in both fresh and cryopreserved samples.

https://doi.org/10.1371/journal.pone.0263869.g006

release most if not all cells [23,47,48]. The resultant cells should have high viability and few aggregates. A dissociation method with high cell yield and cell viability can minimize skin samples and allow detecting cell types with small numbers. A few protocols have been published for preparing single cells from rodent [49–55] and human skins [56–61] via enzymatic digestion and mechanical dissociation. These methods vary in enzyme types and concentrations, digestion time, and temperature [49–61]. Most of them use manual mechanical dissociation, such as dissection, mincing, agitation, pipetting, or passing through syringes that are inefficient and inconsistent. Consequently, the dissociation efficiency and the resultant cell viability, composition vary between methods, publications, and batches. The variations create challenges when comparing scRNA-seq results from different labs. Thus, there is a critical need to develop a standardized single cell preparation method. A standard procedure could be best achieved using validated, commercially available enzyme kits and automated mechanical dissociation devices.

Although we could not find a commercial kit designed explicitly for pig skin, the Miltenyi Human Whole Skin Dissociation Kit and the gentleMACS Dissociator had been used to prepare human skin single cells for scRNA-seq [23,24,27,28,62,63]. Due to the similarity of the human and pig skins, we hypothesized that they could also be used to prepare single pig skin cells. With our protocol, the skin tissue was close to completely dissolved. Only small numbers of cell aggregates were found, and they could be robustly removed with FACS (Fig 1). We were able to isolate $6.0–7.5\times10^4$ viable single cells with a 4-mm full skin biopsy punch. These cells are sufficient for a complete scRNA-seq flow, including cell counting, cell viability, quality assessment, RNA library construction, and quality control.

Reliable methods for preserving single cells make the scRNA-Seq workflow much more flexible and manageable [24,33–36]. A few methods, including cryopreservation in medium containing DMSO, using commercial cell preservation reagent, or methanol fixing, have been reported to preserve single cells [24,33,35,36]. DMSO minimizes forming large intracellular ice crystals, which damage and kill cells. Methanol fixing works through dehydrating cells to preserve nucleic acids in a collapsed form at high concentrations. Upon rehydration, nucleic acids can be restored to their original form and harvested for library preparation [62,64].

Literature research showed the methanol fixing method result in high ambient RNA background and a lower gene expression correlation to un-preserved cells [33]. The same was true for when using commercial CellCover reagent [33]. On the other hand, cryopreserving human and rodent primary cells or cell lines using DMSO plus FBS did not reduce the cell viability and alter the cell composition and gene expression significantly [24,33–36,65]. Our results with pig skin cells (Figs 1–6) agreed well with these literature studies.

In summary, we showed that high-quality single pig skin cells could be generated using the Miltenyi Biotec Whole Skin Dissociation kit and Gentle MACS Dissociator. Single cells could be cryopreserved in 90% FBS+10% DMSO, and the cryopreservation did not significantly alter gene expression and cell compositions. Dead cells and cell aggregates could be removed via FACS before preparing libraries. Using these methods, we obtained high-quality scRNA-Seq data to identify the major skin cell types. The limitation of this study is that only healthy pig skins from young pigs were used. Future studies should test if the protocol works for aged or diseased pig skins.

Supporting information

S1 Fig. Quality control parameters of fresh and cryopreserved (frozen) pig skin cells, including the number of genes, UMIs, and % of mitochondrial gene in each cell. (a) pre-cut-off and (b) post-cut-off data are shown. 4500 genes/cell, 30,000 molecules/cell, and 10% mitochondrial genes are set as the maximum threshold to exclude the doublets, multiples, and low-quality single cells. Each dot represents one cell.
(TIF)

S2 Fig. Clustering analysis of combined (a) and separated (b) fresh and cryopreserved samples shows that the two samples have similar clusters.
(TIF)

S3 Fig. Top 10 marker genes for each cluster.
(TIF)

S4 Fig. Top 10 marker genes for each cell type.
(TIF)

S1 Table. Markers used for annotating cell clusters.
(TIF)

Author Contributions

Conceptualization: Mark A. Carlson, William H. Velander, Yuguo Lei.

Data curation: Li Han, Carlos P. Jara, Rafał K. Wóycicki.

Funding acquisition: Mark A. Carlson, William H. Velander, Marc Libault, Yuguo Lei.

Investigation: Li Han, Carlos P. Jara, Ou Wang, Yu Shi, Xinran Wu, Sandra Thibivilliers.

Project administration: Yuguo Lei.

Supervision: William H. Velander, Eliana P. Araújo, Marc Libault, Chi Zhang, Yuguo Lei.

Writing – original draft: Li Han.

Writing – review & editing: Marc Libault, Chi Zhang, Yuguo Lei.

References

1. Karimkhani C, Dellavalle RP, Coffeng LE, Flohr C, Hay RJ, Langan SM, et al. Global skin disease morbidity and mortality an update from the global burden of disease study 2013. JAMA Dermatology. 2017; 153(5):406–12. https://doi.org/10.1001/jamadermatol.2016.5538 PMID: 28249066

2. Järbrink K, Ni G, Sönnergren H, Schmidtchen A, Pang C, Bajpai R, et al. Prevalence and incidence of chronic wounds and related complications: A protocol for a systematic review. Syst Rev [Internet]. 2016; 5(1):1–6. Available from: https://doi.org/10.1186/s13643-016-0329-y PMID: 27609108

3. Lim HW, Collins SAB, Resneck JS, Bolognia JL, Hodge JA, Rohrer TA, et al. The burden of skin disease in the United States. J Am Acad Dermatol [Internet]. 2017; 76(5):958–972.e2. Available from: https://doi.org/10.1016/j.jaad.2016.12.043 PMID: 28259441

4. Zhang JY. Animal Models of Skin Disorders [Internet]. Second Edi. Animal Models for the Study of Human Disease: Second Edition. Elsevier Inc.; 2017. 357–375 p. Available from: http://dx.doi.org/10.1016/B978-0-12-809468-6/00015-2.

5. Grada A, Mervis J, Falanga V. Research Techniques Made Simple: Animal Models of Wound Healing. J Invest Dermatol. 2018; 138(10):2095–2105.e1. https://doi.org/10.1016/j.jid.2018.08.005 PMID: 30244718

6. Sullivan TP, Eaglstein WH, Davis SC, Mertz P. The pig as a model for human wound healing. Wound Repair Regen. 2001; 9(2):66–76. https://doi.org/10.1046/j.1524-475x.2001.00066.x PMID: 11350644

7. Seaton M, Hocking A, Gibran NS. Porcine models of cutaneous wound healing. ILAR J. 2015; 56(1):127–38. https://doi.org/10.1093/ilar/ilv016 PMID: 25991704

8. Summerfield A, Meurens F, Ricklin ME. The immunology of the porcine skin and its value as a model for human skin. Mol Immunol. 2015; 66(1):14–21. https://doi.org/10.1016/j.molimm.2014.10.023 PMID: 25466611

9. Group FWHCF. Guidance for industry: chronic cutaneous ulcer and burn wounds-developing products for treatment. Wound Repair Regen. 2001; 9:258–68. https://doi.org/10.1046/j.1524-475x.2001.00258.x PMID: 11679134

10. Lamme EN, Druecke D, Steinstraesser L, Hermann S, May PS, Pieper J, et al. Modulation of scar tissue formation using different dermal regeneration templates in the treatment of experimental full-thickness wounds. Wound Repair Regen. 2004; 12(5):518–27. https://doi.org/10.1111/j.1067-1927.2004.012504.x PMID: 15453834

11. Wilbrey-Clark A, Roberts K, Teichmann SA. Cell Atlas technologies and insights into tissue architecture. Biochem J. 2020; 477(8):1427–42. https://doi.org/10.1042/BCJ20190341 PMID: 32339226

12. Moncada R, Barkley D, Wagner F, Chiodin M, Devlin JC, Baron M, et al. Integrating microarray-based spatial transcriptomics and single-cell RNA-seq reveals tissue architecture in pancreatic ductal adenocarcinomas. Nat Biotechnol [Internet]. 2020; 38(3):333–42. Available from: https://doi.org/10.1038/s41587-019-0392-8 PMID: 31932730

13. Ji AL, Rubin AJ, Thrane K, Jiang S, Reynolds DL, Meyers RM, et al. Multimodal Analysis of Composition and Spatial Architecture in Human Squamous Cell Carcinoma. Cell [Internet]. 2020; 182:497–514.e22. Available from: http://www.ncbi.nlm.nih.gov/pubmed/32579974. https://doi.org/10.1016/j.cell.2020.05.039 PMID: 32579974

14. Goltsev Y, Samusik N, Kennedy-Darling J, Bhate S, Hale M, Vazquez G, et al. Deep Profiling of Mouse Splenic Architecture with CODEX Multiplexed Imaging. Cell [Internet]. 2018; 174(4):968–981.e15. Available from: https://doi.org/10.1016/j.cell.2018.07.010 PMID: 30078711

15. Guerrero-juarez CF, Dedhia PH, Jin S, Ruiz-vega R, Ma D, Liu Y, et al. Single-cell analysis reveals fibroblast heterogeneity and myeloid-derived adipocyte progenitors in murine skin wounds. Nat Commun [Internet]. 2019; 10:650. Available from: https://doi.org/10.1038/s41467-018-08247-x PMID: 30737373

16. Tellechea A, Bai S, Dangwal S, Theocharidis G, Nagai M, Koerner S, et al. Topical Application of a Mast Cell Stabilizer Improves Impaired Diabetic Wound Healing. J Invest Dermatol [Internet]. 2020; 140(4):901–911.e11. Available from: https://doi.org/10.1016/j.jid.2019.08.449 PMID: 31568772

17. Chovatiya G, Ghuwalewala S, Walter LD, Cosgrove BD, Tumbar T. High-resolution single-cell transcriptomics reveals heterogeneity of self-renewing hair follicle stem cells. Exp Dermatol. 2020;(December):1–15.

18. Joost S, Annusver K, Jacob T, Sun X, Dalessandri T, Sivan U, et al. The Molecular Anatomy of Mouse Skin during Hair Growth and Rest. Cell Stem Cell. 2020; 26(3):441–457.e7. https://doi.org/10.1016/j.stem.2020.01.012 PMID: 32109378

19. Joost S, Jacob T, Sun X, Annusver K, La Manno G, Sur I, et al. Single-Cell Transcriptomics of Traced Epidermal and Hair Follicle Stem Cells Reveals Rapid Adaptations during Wound Healing. Cell Rep

[Internet]. 2018; 25(3):585–597.e7. Available from: https://doi.org/10.1016/j.celrep.2018.09.059 PMID: 30332640

20. Haensel D, Jin S, Sun P, Cinco R, Dragan M, Nguyen Q, et al. Defining Epidermal Basal Cell States during Skin Homeostasis and Wound Healing Using Single-Cell Transcriptomics. Cell Rep [Internet]. 2020; 30(11):3932–3947.e6. Available from: https://doi.org/10.1016/j.celrep.2020.02.091 PMID: 32187560

21. Vorstandlechner V, Laggner M, Kalinina P, Haslik W, Radtke C, Shaw L, et al. Deciphering the functional heterogeneity of skin fibroblasts using single-cell RNA sequencing. FASEB J. 2020; 34(3):3677–92. https://doi.org/10.1096/fj.201902001RR PMID: 31930613

22. Sinha M, Sen CK, Singh K, Das A, Ghatak S, Rhea B, et al. Direct conversion of injury-site myeloid cells to fibroblast-like cells of granulation tissue. Nat Commun [Internet]. 2018; 9(1):1–19. Available from: https://doi.org/10.1038/s41467-017-02088-w PMID: 29317637

23. Kim D, Chung KB, Kim TG. Application of single-cell RNA sequencing on human skin: Technical evolution and challenges. J Dermatol Sci [Internet]. 2020; 99(2):74–81. Available from: https://doi.org/10.1016/j.jdermsci.2020.06.002 PMID: 32593488

24. Mirizio E, Tabib T, Wang X, Chen W, Liu C, Lafyatis R, et al. Single-cell transcriptome conservation in a comparative analysis of fresh and cryopreserved human skin tissue: pilot in localized scleroderma. Arthritis Res Ther. 2020; 22(1):1–10. https://doi.org/10.1186/s13075-019-2050-4 PMID: 31898524

25. Zou Z, Long X, Zhao Q, Zheng Y, Song M, Ma S, et al. A Single-Cell Transcriptomic Atlas of Human Skin Aging. Dev Cell [Internet]. 2020;1–15. Available from: https://doi.org/10.1016/j.devcel.2020.11.002 PMID: 33238152

26. Cheng JB, Sedgewick AJ, Finnegan AI, Harirchian P, Lee J, Kwon S, et al. Transcriptional Programming of Normal and Inflamed Human Epidermis at Single-Cell Resolution. Cell Rep [Internet]. 2018; 25(4):871–83. Available from: https://doi.org/10.1016/j.celrep.2018.09.006 PMID: 30355494

27. Solé-Boldo L, Raddatz G, Schütz S, Mallm JP, Rippe K, Lonsdorf AS, et al. Single-cell transcriptomes of the human skin reveal age-related loss of fibroblast priming. Commun Biol [Internet]. 2020; 3(1):1–12. Available from: https://doi.org/10.1038/s42003-019-0734-6 PMID: 31925316

28. Xue D, Tabib T, Morse C, Lafyatis R. Transcriptome landscape of myeloid cells in human skin reveals diversity, rare populations and putative DC progenitors. J Dermatol Sci [Internet]. 2020; 97(1):41–9. Available from: https://doi.org/10.1016/j.jdermsci.2019.11.012 PMID: 31836271

29. Hughes TK, Wadsworth MH, Gierahn TM, Do T, Weiss D, Andrade PR, et al. Second-Strand Synthesis-Based Massively Parallel scRNA-Seq Reveals Cellular States and Molecular Features of Human Inflammatory Skin Pathologies. Immunity [Internet]. 2020; 53(4):878–894.e7. Available from: https://doi.org/10.1016/j.immuni.2020.09.015 PMID: 33053333

30. Wang S, Drummond ML, Guerrero-Juarez CF, Tarapore E, MacLean AL, Stabell AR, et al. Single cell transcriptomics of human epidermis identifies basal stem cell transition states. Nat Commun [Internet]. 2020; 11(1). Available from: https://doi.org/10.1038/s41467-020-18075-7 PMID: 32843640

31. Head SR, Kiyomi Komori H, LaMere SA, Whisenant T, Van Nieuwerburgh F, Salomon DR, et al. Library construction for next-generation sequencing: Overviews and challenges. Biotechniques. 2014; 56(2):61–77. https://doi.org/10.2144/000114133 PMID: 24502796

32. Levy SE, Myers RM. Advancements in Next-Generation Sequencing. Annu Rev Genomics Hum Genet. 2016; 17:95–115. https://doi.org/10.1146/annurev-genom-083115-022413 PMID: 27362342

33. Wohnhaas CT, Leparc GG, Fernandez-Albert F, Kind D, Gantner F, Viollet C, et al. DMSO cryopreservation is the method of choice to preserve cells for droplet-based single-cell RNA sequencing. Sci Rep. 2019; 9(1):1–14. https://doi.org/10.1038/s41598-018-37186-2 PMID: 30626917

34. Matson KJE, Sathyamurthy A, Johnson KR, Kelly MC, Kelley MW, Levine AJ. Isolation of adult spinal cord nuclei for massively parallel single-nucleus RNA sequencing. J Vis Exp. 2018; 2018(140):1–12. https://doi.org/10.3791/58413 PMID: 30371670

35. Attar M, Sharma E, Li S, Bryer C, Cubitt L, Broxholme J, et al. A practical solution for preserving single cells for RNA sequencing. Sci Rep [Internet]. 2018; 8(1):1–10. Available from: https://doi.org/10.1038/s41598-017-17765-5 PMID: 29311619

36. Denisenko E, Guo BB, Jones M, Hou R, de Kock L, Lassmann T, et al. Systematic assessment of tissue dissociation and storage biases in single-cell and single-nucleus RNA-seq workflows. Genome Biol. 2020; 21(1):130. https://doi.org/10.1186/s13059-020-02048-6 PMID: 32487174

37. Butler A, Hoffman P, Smibert P, Papalexi E, Satija R. Integrating single-cell transcriptomic data across different conditions, technologies, and species. Nat Biotechnol. 2018; 36(5):411–20. https://doi.org/10.1038/nbt.4096 PMID: 29608179

38. Stuart T, Butler A, Hoffman P, Hafemeister C, Papalexi E, Mauck WM, et al. Comprehensive Integration of Single-Cell Data. Cell [Internet]. 2019; 177(7):1888–1902.e21. Available from: https://doi.org/10.1016/j.cell.2019.05.031 PMID: 31178118

39. Shao X, Liao J, Lu X, Xue R, Ai N, Fan X. scCATCH: Automatic Annotation on Cell Types of Clusters from Single-Cell RNA Sequencing Data. iScience. 2020; 23(3). https://doi.org/10.1016/j.isci.2020.100882 PMID: 32062421

40. Qiu X, Mao Q, Tang Y, Wang L, Chawla R, Pliner HA, et al. Reversed graph embedding resolves complex single-cell trajectories. Nat Methods. 2017; 14(10):979–82. https://doi.org/10.1038/nmeth.4402 PMID: 28825705

41. Trapnell C, Cacchiarelli D, Grimsby J, Pokharel P, Li S, Morse M, et al. The dynamics and regulators of cell fate decisions are revealed by pseudotemporal ordering of single cells. Nat Biotechnol. 2014; 32 (4):381–6. https://doi.org/10.1038/nbt.2859 PMID: 24658644

42. Ji AL, Rubin AJ, Thrane K, Jiang S, Reynolds DL, Meyers RM, et al. Multimodal Analysis of Composition and Spatial Architecture in Human Squamous Cell Carcinoma. J Clean Prod. 2020;1–18.

43. McCarthy DJ, Campbell KR, Lun ATL, Wills QF. Scater: Pre-processing, quality control, normalization and visualization of single-cell RNA-seq data in R. Bioinformatics. 2017; 33(8):1179–86. https://doi.org/10.1093/bioinformatics/btw777 PMID: 28088763

44. McCarthy DJ, Chen Y, Smyth GK. Differential expression analysis of multifactor RNA-Seq experiments with respect to biological variation. Nucleic Acids Res. 2012; 40(10):4288–97. https://doi.org/10.1093/nar/gks042 PMID: 22287627

45. Macosko EZ, Basu A, Satija R, Nemesh J, Shekhar K, Goldman M, et al. Highly parallel genome-wide expression profiling of individual cells using nanoliter droplets. Cell [Internet]. 2015; 161(5):1202–14. Available from: https://doi.org/10.1016/j.cell.2015.05.002 PMID: 26000488

46. Blondel VD, Guillaume JL, Lambiotte R, Lefebvre E. Fast unfolding of communities in large networks. J Stat Mech Theory Exp. 2008; 2008(10).

47. Nguyen QH, Pervolarakis N, Nee K, Kessenbrock K. Experimental Considerations for Single-Cell RNA Sequencing Approaches. 2018; 6(September):1–7.

48. Tung P, Blischak JD, Hsiao CJ, Knowles DA, Burnett JE, Pritchard JK, et al. Batch effects and the effective design of single-cell gene expression studies. Nat Publ Gr [Internet]. 2017;(September 2016):1–15. Available from: https://doi.org/10.1038/srep39921 PMID: 28045081

49. Cha ST, Talavera D, Demir E, Nath AK, Sierra-Honigmann MR. A method of isolation and culture of microvascular endothelial cells from mouse skin. Microvasc Res. 2005; 70(3):198–204. https://doi.org/10.1016/j.mvr.2005.08.002 PMID: 16188282

50. Eidsmo L, Allan R, Caminschi I, van Rooijen N, Heath WR, Carbone FR. Differential Migration of Epidermal and Dermal Dendritic Cells during Skin Infection. J Immunol. 2009; 182(5):3165–72. https://doi.org/10.4049/jimmunol.0802950 PMID: 19234214

51. King IL, Kroenke MA, Segal BM. GM-CSF-dependent, CD103+ dermal dendritic cells play a critical role in Th effector cell differentiation after subcutaneous immunization. J Exp Med. 2010; 207(5):953–61. https://doi.org/10.1084/jem.20091844 PMID: 20421390

52. Farina GA, York MR, Di Marzio M, Collins CA, Meller S, Homey B, et al. Poly(I:C) drives type i IFN- and TGFB-mediated inflammation and dermal fibrosis simulating altered gene expression in systemic sclerosis. J Invest Dermatol [Internet]. 2010; 130(11):2583–93. Available from: https://doi.org/10.1038/jid.2010.200 PMID: 20613770

53. Antsiferova M, Martin C, Huber M, Feyerabend TB, Förster A, Hartmann K, et al. Mast Cells Are Dispensable for Normal and Activin-Promoted Wound Healing and Skin Carcinogenesis. J Immunol. 2013; 191(12):6147–55. https://doi.org/10.4049/jimmunol.1301350 PMID: 24227781

54. Gu D, Fan Q, Xie J. Cell population analyses during skin carcinogenesis. J Vis Exp. 2013;(78):e50311. https://doi.org/10.3791/50311 PMID: 23995436

55. Rinkevich Y, Walmsley GG, Hu MS, Maan ZN, Newman AM, Drukker M, et al. Identification and isolation of a dermal lineage with intrinsic fibrogenic potential. Science (80-). 2015; 348(6232). https://doi.org/10.1126/science.aaa2151 PMID: 25883361

56. Zheng Y, Nace A, Chen W, Watkins K, Sergott L, Homan Y, et al. Mature hair follicles generated from dissociated cells: A universal mechanism of folliculoneogenesis. Dev Dyn. 2010; 239(10):2619–26. https://doi.org/10.1002/dvdy.22398 PMID: 21038446

57. Huschtscha LI, Napier CE, Noble JR, Bower K, Au AYM, Campbell HG, et al. Enhanced isolation of fibroblasts from human skin explants. Biotechniques. 2012; 53(4):239–44. https://doi.org/10.2144/0000113939 PMID: 23046507

58. Nagel S, Rohr F, Weber C, Kier J, Siemers F, Kruse C, et al. Multipotent Nestin-Positive Stem Cells Reside in the Stroma of Human Eccrine and Apocrine Sweat Glands and Can Be Propagated Robustly In Vitro. PLoS One. 2013; 8(10):1–14. https://doi.org/10.1371/journal.pone.0078365 PMID: 24205211

59. Cheuk S, Wikén M, Blomqvist L, Nylén S, Talme T, Ståhle M, et al. Epidermal Th22 and Tc17 Cells Form a Localized Disease Memory in Clinically Healed Psoriasis. J Immunol. 2014; 192(7):3111–20. https://doi.org/10.4049/jimmunol.1302313 PMID: 24610014

60. Botting RA, Bertram KM, Baharlou H, Sandgren KJ, Fletcher J, Rhodes JW, et al. Phenotypic and functional consequences of different isolation protocols on skin mononuclear phagocytes. J Leukoc Biol. 2017; 101(6):1393–403. https://doi.org/10.1189/jlb.4A1116-496R PMID: 28270408

61. Chen Z, Wang X, Jin T, Wang Y, Hong CS, Tan L, et al. Increase in the radioresistance of normal skin fibroblasts but not tumor cells by mechanical injury. Cell Death Dis. 2017; 8(2).

62. Meeson A, Fuller A, Breault DT, Owens WA, Richardson GD. Optimised Protocols for the Identification of the Murine Cardiac Side Population. Stem Cell Rev Reports. 2013; 9(5):731–9. https://doi.org/10.1007/s12015-013-9440-9 PMID: 23619929

63. Baldan V, Griffiths R, Hawkins RE, Gilham DE. Efficient and reproducible generation of tumour-infiltrating lymphocytes for renal cell carcinoma. Br J Cancer. 2015; 112(9):1510–8. https://doi.org/10.1038/bjc.2015.96 PMID: 25867267

64. Wang X, Yu L, Wu A. Effect of methanol fixation on single-cell RNA sequencing data. 2020;(1).

65. Denisenko E, Guo BB, Jones M, Hou R, de Kock L, Lassmann T, et al. Systematic assessment of tissue dissociation and storage biases in single-cell and single-nucleus RNA-seq workflows. bioRxiv. 2019;1–25.